Nigerian Journal of Physics (NJP)
ISSN online: 3027-0936
ISSN print: 1595-0611
DOI: https://doi.org/10.62292/njp.v35(S).2026.763
Volume 35(S), November 2026

Stochastic Facies Architecture, Spatial Anisotropy, and Implications for Potential Reservoir Connectivity in a Heterogeneous Fluvio-Deltaic System, Onshore Niger Delta, Nigeria

Joseph C. Chinaka[1], Ikechukwu E. Nwosu[1], Okechukwu K. Nwofor[1], Ifeanyi I. C. Agbodike[1], B. C. Ejiogu[2], Ijeoma L. David-Okoro[3]

[1]Department of Physics, Imo State University, Owerri, Imo State, Nigeria
[2]Department of Physics, Alvan Ikoku Federal University of Education, Owerri, Imo State
[3]Department of Physics and Industrial Physics, Nnamdi Azikiwe University, Awka, Anambra State, Nigeria.

*Corresponding Author's Email: jcchinaka@imsuonline.edu.ng Phone No.: +2348060384511

Keywords:
Stochastic facies modelling, Spatial anisotropy, Reservoir connectivity, Fluvio-deltaic reservoirs, Niger Delta.

Submitted: 20/10/2026

Accepted: 28/10/2026

Published: 6/11/2026

ABSTRACT

Reservoir connectivity in fluvio-deltaic systems depends on the spatial arrangement of sand bodies and shale barriers. This study examines the potential static geological connectivity of the C2000–D1000 and D1000–D2000 intervals in the Chinak Field, onshore Niger Delta, using well logs, seismic interpretation, structural modelling, variogram analysis, and Sequential Indicator Simulation. The available modelled net-to-gross (NTG) ranges are 0.53882–0.95224 for C2000–D1000 and 0.47117463–0.99902231 for D1000–D2000. Fitted horizontal variogram ranges of 1,234 m and a vertical range of 3.9 m give a horizontal-to-vertical correlation-range ratio of approximately 316.4. The facies-model illustrations suggest potentially greater lateral sand-body continuity in C2000–D1000 and more channel-scale variability and possible compartmentalization in D1000–D2000. These are qualitative interpretations of potential static connectivity, not measurements of connected sand volumes or evidence of dynamic fluid communication. The absence of cell-level facies-grid exports prevented calculation of component counts, largest connected components, connected sand fractions, and uncertainty across realizations.

INTRODUCTION

Reservoir heterogeneity fundamentally controls hydrocarbon storage, fluid communication, sweep efficiency, and ultimately reservoir performance. This control is particularly pronounced in fluvio-deltaic successions, where repeated changes in depositional energy, sediment supply, channel migration, abandonment, and marine influence generate complex arrangements of sandstone, shaly sand, and shale over relatively short lateral and vertical distances. In the Niger Delta, stacked Agbada Formation reservoirs commonly preserve such heterogeneity at multiple scales, with facies architecture influenced by both depositional processes and syn-depositional structural development (Kuye & Hampson, 2023).

Reservoir connectivity within these systems depends not only on the proportion of reservoir-quality sand but also on its geometry, orientation, continuity, and spatial relationship with non-reservoir facies. Laterally connected sand bodies may establish preferential pathways for pressure and fluid communication. In contrast, shale interbeds, mud-rich margins, and discontinuous sand bodies can act as baffles or barriers and generate vertical or lateral compartmentalization. Integrated analysis of Niger Delta reservoirs has similarly demonstrated that sedimentological heterogeneity can either enhance communication through sand-to-sand contacts or restrict flow where mud barriers interrupt reservoir continuity (Spina et al., 2023; Spina et al., 2025). In this study, reservoir connectivity refers principally to static geological connectivity, defined by the spatial continuity, linkage, and compartmentalization of reservoir-quality sand bodies within the stochastic facies framework.

Three-dimensional stochastic modelling provides an appropriate framework for representing this complexity because it preserves spatial variability rather than reducing geological architecture to a single

deterministic configuration. Sequential Indicator Simulation (SIS) is particularly suited to categorical facies distributions, whereas Sequential Gaussian Simulation (SGS) can reproduce continuous petrophysical variability conditioned to well data and spatial-continuity models. Recent high-resolution modelling of heterogeneous clastic reservoirs has demonstrated that integrating SIS-derived lithofacies with SGS-derived petrophysical properties can preserve spatial geological variability and generate alternative geologically plausible reservoir configurations (Al-Mudhafar et al., 2024).

A critical component of such modelling is spatial anisotropy. Facies continuity is rarely equal in all directions; depositional processes commonly generate preferential orientations in which correlation lengths are substantially greater along depositional or sediment-transport trends than perpendicular to them, while vertical continuity is restricted by stratification and shale interbeds. Variogram-defined major, minor, and vertical ranges therefore provide more than statistical parameters: they encode directional geological continuity that can influence the geometry and connectivity of simulated reservoir bodies. Consequently, two reservoirs with comparable sand proportions may exhibit very different connectivity if their sand bodies differ in anisotropy, lateral persistence, vertical stacking, or interruption by shale.

This issue is especially relevant in the Niger Delta, where recent three-dimensional reservoir studies continue to demonstrate pronounced spatial variability in facies and petrophysical properties and emphasize the need for integrated seismic, well-log, structural, and geostatistical modelling (Oyesomi et al., 2025). However, many reservoir-characterization studies emphasize property distribution, reservoir quality, or hydrocarbon volumes, while the explicit relationship among stochastic facies architecture, directional anisotropy, and reservoir connectivity remains less frequently quantified.

Recent articles in the Nigerian Journal of Physics provide complementary evidence for integrated reservoir characterization in the Niger Delta. Olaoluwa et al. (2025) used well-log-derived petrophysical parameters to characterize reservoir intervals in the Abig Field, while Igonoh et al. (2026) combined petrophysical evaluation, seismic attributes, and amplitude-versus-offset modelling in the JASMI Field. These studies support integrating multiple subsurface datasets to characterize reservoir properties and structural context. However, neither study provides connected-component measurements for the Chinak Field, so their findings do not independently validate the static connectivity interpretations presented here.

Despite increasing application of stochastic facies modelling, an important uncertainty remains in how simulated facies geometry and directional spatial continuity translate into effective reservoir connectivity. Facies proportions alone do not uniquely determine connectivity because geometrically different stochastic realizations may contain similar proportions of reservoir facies while exhibiting markedly different degrees of sand-body linkage and compartmentalization. Recent studies have therefore emphasized connectivity as an independent attribute of geological heterogeneity that should be evaluated explicitly rather than inferred solely from facies abundance or petrophysical quality (Manzocchi et al., 2023; Jin et al., 2024). This distinction is particularly important in fluvio-deltaic systems, where anisotropic channel and sand-body geometries can promote preferential connectivity along depositional trends while shale interbeds and lateral facies transitions restrict communication perpendicular to those trends. However, the combined control of stochastic facies architecture and directional anisotropy on connectivity remains insufficiently quantified in stacked Niger Delta reservoirs.

The Chinak Field provides a setting for examining how facies architecture and variogram-defined spatial continuity may influence static geological connectivity. This study compares the C2000–D1000 and D1000–D2000 intervals using available SIS facies-model illustrations and reported NTG ranges. Its contribution is an integrated, model-based interpretation of potential sand-body linkage and compartmentalization, rather than a quantitative measurement of connected sand volumes.

Geological Setting and Study Area

The established threefold subdivision of the Niger Delta into the Akata, Agbada and Benin formations provides the regional stratigraphic framework for this study. Short and Stäuble (1967) described this succession and its petroleum significance, while Reijers (2011) examined its sedimentological evolution and internal stratigraphic variability.

The Chinak Field is situated in the Warri area of Delta State, southern Nigeria, within the onshore Niger Delta petroleum province and the central swamp depobelt. The study area is located at 5.52° N latitude and 5.75° E longitude, which are the area coordinates. This position places the field within the north-central onshore Niger Delta.

The Niger Delta occupies the continental margin of the Gulf of Guinea and extends approximately between latitudes 3° and 6° N and longitudes 3° and 9° E, covering an area of about 75,000 km². The basin is bounded broadly by the Benin flank to the northwest, the Calabar flank to the east, the Anambra Basin–Abakaliki High to the north, and the Gulf of Guinea to the south. Its geological evolution reflects sustained sediment supply, rapid subsidence, and gravity-driven

deformation, resulting in a thick progradational clastic succession characterized by growth faults, rollover structures, and laterally variable sandstone–shale sequences. These features have made the Niger Delta one of Africa's major hydrocarbon provinces and have strongly influenced reservoir architecture, connectivity, and compartmentalization. Recent studies continue to emphasize the value of integrating seismic interpretation, well-log analysis, and three-dimensional reservoir modelling for resolving this complexity within Niger Delta reservoirs (Adeogun et al., 2025; Attouman et al., 2025).

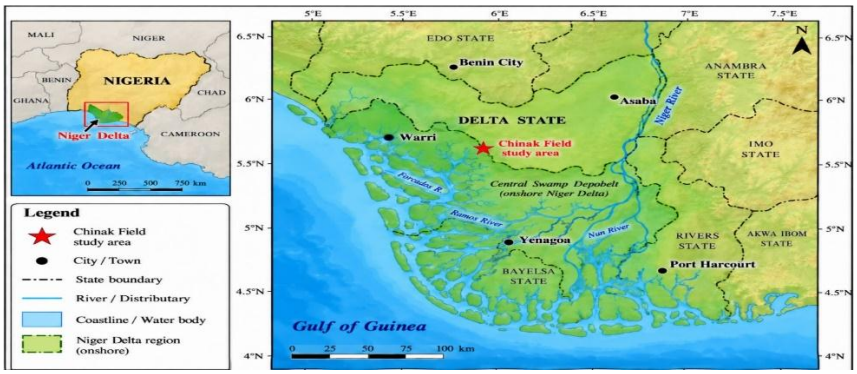


Figure 1: Location map of the Niger Delta, southern Nigeria, showing Delta State, Warri, the approximate Chinak Field study area around 5.52° N, 5.75° E, the central swamp depobelt, and the regional boundaries of the Niger Delta Basin

Stratigraphically, the Niger Delta consists of a thick Cenozoic clastic wedge traditionally divided into the Akata, Agbada and Benin formations. The basal Akata Formation is dominated by marine and prodelta shales and constitutes the principal source-rock interval. It is overlain by the Agbada Formation, a paralic succession of interbedded sandstone and shale deposited under fluvial, deltaic, coastal and shallow-marine conditions. The upper Benin Formation consists predominantly of continental sands deposited mainly in fluvial and upper coastal-plain environments. Recent Niger Delta studies continue to recognize the Agbada Formation as the principal petroleum-bearing interval, with sandstone bodies providing the main reservoirs and interbedded shales acting as local seals and flow barriers (Adeogun et al., 2025; Attouman et al., 2025; Oyesomi et al., 2025).

The reservoirs investigated in the Chinak Field occur within the Agbada Formation and comprise stacked fluvio-deltaic sandstone bodies separated locally by shaly-sand and shale intervals. Their architecture reflects repeated phases of sediment progradation, channel development, abandonment, and marine influence, producing strong lateral and vertical facies variability. Such depositional organization is particularly important to the present study because sand-body continuity may promote reservoir connectivity, whereas shale interbeds and heterolithic intervals can restrict vertical communication and create internal compartmentalization. Similar Niger Delta modelling studies have demonstrated that spatial variations in facies distribution and reservoir geometry strongly influence hydrocarbon distribution and reservoir connectivity (Oyesomi et al., 2025; Attouman et al., 2025).

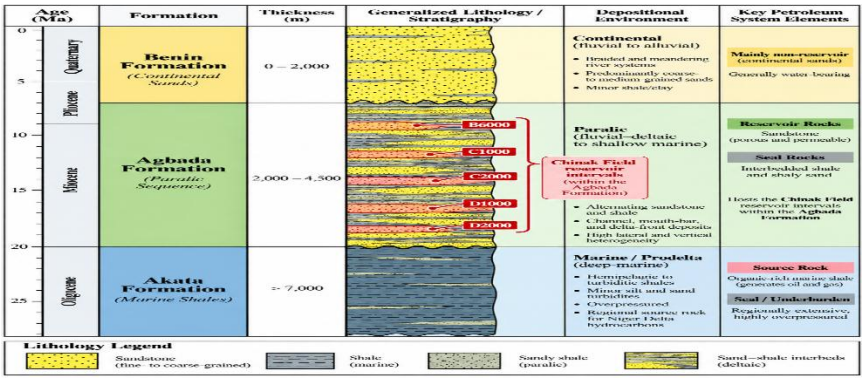


Figure 2. Generalized stratigraphic column of the Niger Delta showing the Akata, Agbada, and Benin formations and the stratigraphic position of the Chinak Field reservoir intervals within the Agbada Formation

Structurally, deformation in the Niger Delta is dominated by gravity-driven extensional tectonics associated with rapid sediment loading and movement above under-compacted Akata shales. This structural style commonly produces listric growth faults, rollover anticlines, and subsidiary synthetic and antithetic faults that exert strong controls on trap geometry and reservoir compartmentalization. Recent seismic studies continue to document growth faults and rollover structures as major controls on Niger Delta hydrocarbon accumulation and reservoir segmentation (Adeogun et al., 2025; Attouman et al., 2025). Fault architecture can also influence reservoir communication, with recent work showing that faults may produce compartmentalized and directionally anisotropic fluid-flow behaviour in Niger Delta reservoirs (Spina et al., 2025).

Within the Chinak Field, the structural configuration is characterized by a rollover anticline bounded to the north by a major growth fault and accompanied by a minor antithetic crestal fault. The fold is relatively low relief, with gentle flanks and a broadly flattened crest, while its axis changes position with depth, approximately parallel to the bounding growth fault. These structures provide the framework within which the stacked reservoir intervals occur and may interact with depositional heterogeneity to influence lateral sand-body continuity and compartmentalization. The present study therefore evaluates connectivity principally within this combined stratigraphic and structural framework, with particular emphasis on the stochastic arrangement of sand, shaly-sand and shale facies and their variogram-defined directional continuity.

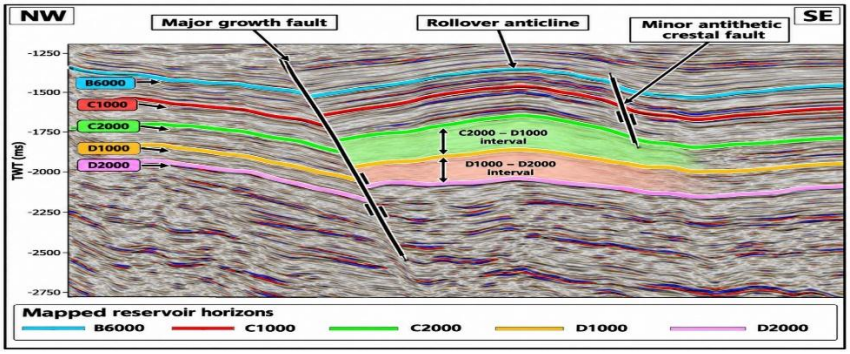


Figure 3. Representative seismic section through the Chinak Field showing the major growth fault, minor antithetic crestal fault, rollover anticline, and interpreted reservoir horizons. The C2000–D1000 and D1000–D2000 intervals represent the principal stratigraphic domains investigated in this study

MATERIALS AND METHODS

Data and Modelling Framework

The study integrated wireline logs from five wells (Chinak-023, Chinak-031, Chinak-033, Chinak-035 and Chinak-038), three-dimensional seismic data, check-shot information, interpreted reservoir horizons, and existing geological-model outputs from the Chinak Field. The wireline suite included gamma-ray, resistivity, density, neutron, sonic, and caliper logs, which were quality-controlled and depth-matched before interpretation. Three-dimensional seismic data provided the structural framework and lateral control away from the wells, while check-shot data were used for well-to-seismic calibration and time–depth conversion. All seismic interpretation, well-to-seismic integration, structural modelling, facies upscaling, variogram analysis, Sequential Indicator Simulation, and reservoir-connectivity modelling were performed using Schlumberger Petrel 2017.

Structural and Stratigraphic Framework

Reservoir horizons were correlated from well logs and tied to the 3-D seismic volume using check-shot-calibrated well information. Horizon and fault interpretation defined the principal growth fault, subsidiary antithetic faulting, and rollover geometry of the field. The interpreted surfaces were subsequently used to construct the three-dimensional stratigraphic framework, including zonation and layering required for facies simulation. Particular attention was given to the stacked C2000–D1000 and D1000–D2000 intervals, which constitute the principal domains for the facies-connectivity analysis.

Grid Definition, Zonation and Layering

A three-dimensional corner-point grid was constructed in Petrel using the interpreted reservoir horizons and fault framework as structural constraints. The X–Y grid provided the lateral discretization for integration of seismic, well, and reservoir-property data.

Grid Dimensions and Spatial Resolution

The three-dimensional geological model was discretized into 100 cells along the X-axis, 100 cells along the Y-axis, and 175 stratigraphic layers along the vertical (Z) axis (NX = 100, NY = 100, NZ = 175). The total number of grid cells was calculated by multiplying the number of cells along the three axes (NX × NY × NZ), giving 100 × 100 × 175 = 1,750,000 cells. This value represents the total number of cells in the geological grid before excluding inactive cells associated with structural boundaries and areas outside the modelled reservoir volume. The vertical layers follow the interpreted reservoir geometry and accommodate variations in stratigraphic thickness across the model.

The gross thickness of the modelled intervals varies spatially across the field. Based on correlated reservoir tops, the C2000–D1000 interval is approximately 160–185 m thick, with a representative thickness of about 175 m, whereas the D1000–D2000 interval is approximately 30–75 m thick, averaging about 55 m. The model was vertically subdivided into stratigraphic layers to represent variations in reservoir thickness and facies architecture. However, the available grid summaries do not permit independent verification of vertical cell resolution relative to the fitted 3.9 m variogram range.

Geological zonation was defined using the interpreted stratigraphic boundaries of the reservoir intervals. The C2000–D1000 and D1000–D2000 intervals were treated as separate modelling zones. Additional geometric layers were inserted within each zone to improve vertical resolution without introducing new geological boundaries.

Facies Classification and Stochastic Simulation

Indicator-based geostatistical approaches provide a basis for representing categorical spatial distributions without assuming a Gaussian variable (Journel, 1983). However, a variogram-based simulation does not necessarily reproduce complex curvilinear channel geometry; Strebelle (2002) demonstrated how multiple-point statistics can represent geological patterns that extend beyond two-point spatial relationships. The present study used SIS rather than multiple-point simulation.

Lithofacies were classified into three reservoir-relevant categories: sand, shaly sand, and shale—using gamma-ray-derived shale volume (V_{sh}) as the principal discriminator, supported by neutron-density responses where available. For reproducible facies assignment, clean sand was defined as $V_{sh} < 0.10$, shaly sand as $0.10 \leq V_{sh} < 0.30$, and shale as $V_{sh} \geq 0.30$. These thresholds are consistent with the low shale contents observed in the cleaner Chinak reservoir intervals and with published classifications of Agbada Formation lithofacies in the Niger Delta. Low gamma-ray and V_{sh} values therefore represent clean reservoir sand, intermediate values represent clay-bearing transitional facies, and values of 0.30 or greater represent shale-dominated intervals.

Shale volume was derived from the gamma-ray index using the Larionov relationship for Tertiary rocks:

$$I_{GR} = \frac{GR_{log} - GR_{min}}{GR_{max} - GR_{min}} \quad (1)$$

$$V_{sh} = 0.083(2^{3.7I_{GR}} - 1) \quad (2)$$

Where GR_{log} is the measured gamma-ray response, and GR_{min} and GR_{max} represent the clean-sand and shale baselines, respectively. The classified facies logs were subsequently upscaled to the geological grid and used as conditioning data for Sequential Indicator Simulation.

Facies-Log Upscaling

Before stochastic simulation, the discrete facies logs were upscaled to the three-dimensional geological grid in Petrel using a dominant-facies method. For each grid cell intersected by a well trajectory, the cumulative thickness of log samples classified as sand, shaly sand, and shale was determined, and the cell was assigned the facies occupying the greatest proportion of the intersected interval. Upscaling was performed separately within the C2000–D1000 and D1000–D2000 stratigraphic zones, thereby preventing facies samples from being mixed across reservoir boundaries. This approach preserved the categorical character of the facies data and avoided numerical averaging of discrete facies codes. The upscaled facies logs were checked against the original well-log interpretation to ensure preservation of the principal vertical facies proportions and transitions, and the resulting grid-cell facies were used as hard conditioning data for Sequential Indicator Simulation.

Facies distributions were generated using Sequential Indicator Simulation (SIS) to preserve categorical proportions and variogram-defined spatial continuity while honouring the upscaled well observations (Deutsch & Journel, 1998; Pyrcz & Deutsch, 2014).

Model Conditioning

The stochastic facies simulations were conditioned jointly to the well-derived facies data and the three-dimensional structural framework. The quality-controlled well trajectories were positioned within the geological grid using the available deviation-survey information, and the upscaled facies values from Chinak-023, Chinak-031, Chinak-033, Chinak-035 and Chinak-038 were treated as hard conditioning data.

Consequently, simulated facies at grid cells intersected by the wells honoured the observed sand, shaly-sand and shale assignments rather than being replaced by unconditional simulated values. Accurate well positioning was particularly important because the well observations constitute the fixed spatial control to which the stochastic model was anchored.

The structural limits of the simulation were defined by depth-converted reservoir horizons and interpreted fault surfaces derived from the three-dimensional seismic interpretation. Reservoir tops and bases, calibrated to the wells through check-shot-based well-to-seismic ties, defined the upper and lower boundaries of each modelling interval and restricted facies simulation to the corresponding reservoir volume. This prevented simulated facies from propagating beyond the interpreted stratigraphic limits. Fault surfaces were incorporated explicitly into the structural framework and subdivided the model into structurally coherent fault blocks while preserving interpreted reflector offsets and reservoir geometry. Accordingly, the C2000–D1000 and D1000–D2000 intervals were simulated within their respective stratigraphic and structural domains, with facies away from the wells generated according to the conditioning data, facies proportions, and variogram-defined spatial continuity.

SIS Simulation Settings

Sequential Indicator Simulation was used to model facies separately in the C2000–D1000 and D1000–D2000 zones, conditioned to well facies and the fitted variogram geometry. The source presentation documents SIS facies models but does not verify the number of saved realizations or provide cell-level realizations for statistical uncertainty analysis. Accordingly, no realization count or realization-based uncertainty estimate is asserted here.

Facies proportions were treated as locally varying in the vertical direction to preserve the stratigraphic variation observed in the upscaled well data and the stacked character of the Agbada succession. Separate facies-proportion distributions were therefore applied within the C2000–D1000 and D1000–D2000 zones. In the absence of evidence for an independently defined lateral probability trend, facies proportions were assumed to be stationary laterally within each stratigraphic zone. The SIS procedure was configured to honour the upscaled well facies as hard conditioning data and reproduce the specified facies proportions and variogram-defined spatial continuity. However, the absence of realization-specific outputs prevented independent verification of these properties across individual simulations.

Variogram analysis and spatial anisotropy

Experimental indicator variograms were used to quantify directional facies continuity before stochastic simulation. The variograms were fitted with a spherical model in Petrel. The adopted model had major and minor horizontal ranges of 1234 m and a vertical range of 3.9 m. These values correspond to a major-to-minor anisotropy ratio of 1.00 and a major-to-vertical anisotropy ratio of approximately 316.41. The identical major and minor ranges indicate essentially isotropic continuity within the horizontal plane, whereas the much shorter vertical range demonstrates pronounced horizontal-to-vertical anisotropy. The fitted variogram parameters were used to constrain Sequential Indicator Simulation so that the simulated facies architecture honoured the well-conditioning data and the measured spatial continuity.

Table 1: Variogram Parameters used to Constrain Facies Spatial Continuity

Parameter	Value	Unit
Variogram model	Spherical	–
Major range	1234	m
Minor range	1234	m
Vertical range	3.9	m
Major/minor anisotropy ratio	1.00	–
Major/vertical anisotropy ratio	316.41	–

Reservoir-connectivity assessment

Larue and Hovadik (2006) distinguished sand-body connectivity from reservoir connectivity to wells and demonstrated the importance of connected geological bodies in channelized reservoirs. This distinction supports treating the displayed SIS facies geometries as evidence of potential pathways, rather than as quantified connected fractions or demonstrated well-to-well communication.

Potential static geological connectivity was interpreted qualitatively from the three-dimensional SIS facies-model illustrations, the arrangement of sand, shaly sand, and shale, and variogram-defined spatial continuity. Clean sand was treated as a potential reservoir pathway, shaly sand as a possible baffle, and shale as a potential barrier. The available material does not contain cell-level facies arrays, so connected-component measurements were not performed.

For a future quantitative assessment, a connected sand component would comprise clean-sand cells sharing a face along X, Y, or Z, excluding edge-only and corner-only contacts. This six-neighbour rule defines a

proposed reproducible calculation, not a measurement completed in the present study.

Shale interbeds and shaly-sand transitions were interpreted as possible impediments to sand-body continuity. Their effectiveness as hydraulic barriers was not tested using pressure, production, or tracer observations.

Potential compartments were inferred where the displayed facies architecture suggested sand-body termination or separation by heterolithic units or faults. No counts or volumes of isolated sand components were calculated.

Table 2: Proposed Operational Criteria for Future Quantitative Assessment of Static Reservoir Connectivity

Feature	Operational criterion
Connected sand body	Face-connected cluster of clean-sand cells; edge/corner contact excluded
Lateral connection	Same sand component continues through adjacent X-Y cells
Vertical connection	Same sand component continues through successive Z layers
Shaly-sand baffle	Shaly-sand cell interrupts clean-sand continuity but is not treated as a complete barrier
Shale barrier	Contiguous shale cells interrupt a clean-sand pathway laterally or vertically
Compartmentalized zone	Two or more clean-sand components with no face-connected clean-sand path between them
Fault-bounded compartment	Separate structural block unless the model explicitly preserves sand-to-sand continuity across the fault

These criteria define a proposed connectivity-analysis procedure and were not applied to cell-level facies grids in the present study.

Comparative Analysis

The two model domains were compared in terms of sand-body continuity, degree of vertical stacking, lateral termination, shale-barrier development and dominant direction of spatial continuity. Interpretations were restricted to features directly supported by the stochastic facies architecture and variogram structure; dynamic communication was not inferred in the absence of production, pressure, or tracer data. The comparative analysis therefore provides a qualitative geological assessment of how stochastic facies architecture and directional spatial anisotropy may influence potential static reservoir connectivity within the stacked fluvio-deltaic succession.

RESULTS AND DISCUSSION

Stochastic Facies Architecture and Structural Framework

Sequential Indicator Simulation reproduced a heterogeneous three-dimensional distribution of sand, shaly sand, and shale within the C2000–D1000 and D1000–D2000 intervals. In both domains, reservoir-quality sand occurs as spatially variable bodies rather than as laterally uniform sheets, while shaly-sand and shale facies interrupt sand continuity to varying degrees. The resulting architecture is consistent with the heterolithic character expected of the paralic Agbada Formation and demonstrates that reservoir connectivity depends on the spatial arrangement of facies rather than on sand abundance alone. This interpretation agrees with recent stochastic studies showing that SIS-based facies models can preserve geologically meaningful sand–shale architecture in heterogeneous clastic reservoirs (Al-Mudhafar et al., 2024).

At field scale, the mapped rollover anticline and associated growth and antithetic faults provide the structural framework within which the facies bodies occur. These structures may impose additional compartment boundaries, whereas intra-reservoir communication is governed principally by sand-body linkage and the distribution of intervening shale. Comparable Niger Delta studies demonstrate that structural and sedimentological heterogeneities commonly operate together to determine reservoir communication (Spina et al., 2023, 2025).

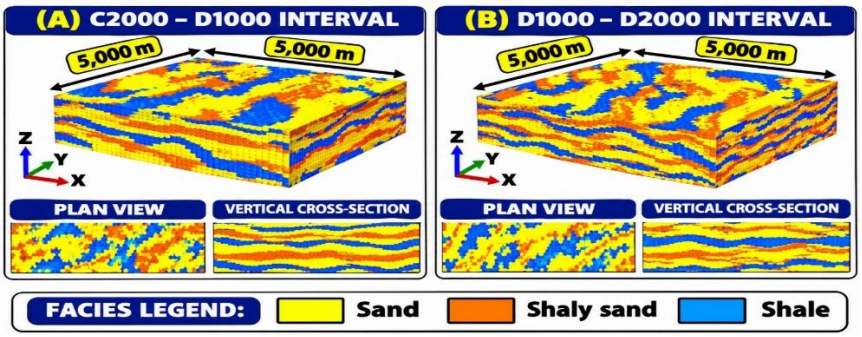


Figure 4. Comparative three-dimensional Sequential Indicator Simulation (SIS) facies illustrations of the C2000–D1000 (a) and D1000–D2000 (b) reservoir intervals, Chinak Field, onshore Niger Delta. The plan views and vertical cross-sections illustrate the spatial distribution of sand, shaly sand, and shale facies. The illustrations provide qualitative comparisons of facies architecture; vertical dimensions are schematic and should not be interpreted as measured reservoir thicknesses

Connectivity architecture of the C2000–D1000 interval

The C2000–D1000 facies illustrations show laterally variable, locally stacked sand bodies interspersed with shaly sand and shale. This arrangement suggests possible lateral linkage and interruptions to vertical continuity, but it does not establish a measured connectivity level.

The C2000–D1000 interval is therefore interpreted as having geological potential for laterally preferential sand-body linkage, with possible vertical baffles. This is a qualitative model-based interpretation, not a measured classification of reservoir connectivity.

Connectivity architecture of the D1000–D2000 interval

The D1000–D2000 facies illustrations suggest channel-influenced, variably stacked sand bodies and lateral terminations within a heterolithic background. These features may influence potential static connectivity, but their connected volumes remain unquantified.

Vertically, clean sand is locally succeeded by shaly sand and shale, producing repeated interruptions to reservoir continuity. These shale intervals provide potential intra-reservoir barriers and create conditions favourable for stratigraphic compartmentalization. The underlying facies interpretation further indicates stronger lateral than vertical continuity, consistent with an anisotropic fluvio-deltaic architecture in which stratification and shale lamination restrict vertical linkage.

The reported modelled NTG range of 0.47117463–0.99902231 is wider than the 0.53882–0.95224 range for C2000–D1000. This describes variability in the modelled NTG property; it does not establish a measured difference in connected sand volume or compartment counts.

Quantitative Results and Interpretation of Potential Reservoir Connectivity

Table 3 presents the reported minimum, maximum, and range of net-to-gross (NTG) values for the C2000–D1000 and D1000–D2000 reservoir intervals. These values were obtained from the available reservoir modelling summaries. However, the source records do not establish whether the reported extrema represent individual grid-cell values, stratigraphic-layer averages, spatial summaries, or variation across stochastic realizations. Consequently, the NTG ranges are treated as descriptive statistics of the reported model outputs rather than measures of realization uncertainty or reservoir connectivity.

Table 3: Reported minimum, maximum, and range of net-to-gross (NTG) values for the C2000–D1000 and D1000–D2000 reservoir intervals, Chinak Field, onshore Niger Delta, Nigeria

Parameter	C2000–D1000	D1000–D2000
Minimum NTG	0.53882	0.47117
Maximum NTG	0.95224	0.99902
NTG range	0.41342	0.52785

The D1000–D2000 interval exhibits a wider reported NTG range (0.52785) than the C2000–D1000 interval (0.41342), suggesting a potentially greater spread in the reported reservoir proportions. Although this difference may reflect variations in reservoir heterogeneity between the two intervals, the statistical basis of the reported NTG extrema remains unverified. Consequently, the wider range cannot independently establish greater geological heterogeneity in the D1000–D2000 interval, particularly without confirmation that

both ranges were derived using comparable aggregation procedures. Furthermore, NTG variability does not directly quantify sand-body connectivity. Interpretations of potential static geological connectivity and compartmentalization therefore rely on the combined assessment of modelled facies architecture, sand-body distribution, and spatial correlation characteristics rather than measured connected sand-body volumes.

Spatial Anisotropy and Its Implications for Potential Static Reservoir Connectivity

The fitted variogram ranges characterize directional spatial correlation, but a variogram alone cannot establish the connectivity of individual sand bodies. Strebelle (2002) showed that curvilinear geological patterns may require spatial information beyond conventional two-point statistics. Accordingly, the horizontal-to-vertical range ratio reported here should not be interpreted as a connected-volume fraction.

Variogram analysis provides quantitative evidence of strongly scale-dependent spatial continuity within the modelled facies architecture. A spherical variogram model was fitted with major and minor horizontal ranges of 1234 m and a vertical range of only 3.9 m (Table 1).

The anisotropy ratios are:

$$A_h = \frac{R_{major}}{R_{minor}} = \frac{1234}{1234} = 1.00 \quad (3)$$

and

$$A_v = \frac{R_{major}}{R_{vertical}} = \frac{1234}{3.9} \approx 316.41 \quad (4)$$

The major-to-minor range ratio is therefore 1.00, indicating approximately equal spatial continuity in the two horizontal directions represented by the fitted variogram. In contrast, the major-to-vertical range ratio is approximately 316.4, demonstrating a pronounced contrast between horizontal and vertical facies continuity.

This result reveals that the dominant anisotropy in the Chinak reservoir architecture is principally horizontal–vertical rather than within the horizontal plane. The fitted variogram model indicates a horizontal spatial correlation range of approximately 1.23 km, compared with a vertical range of 3.9 m. These values characterize the directional scales of spatial correlation within the modelled facies distribution and do not necessarily represent the physical extent or uninterrupted continuity of individual sand bodies. Such a large disparity is consistent with the strongly stratified architecture of fluvio-deltaic deposits, where laterally persistent sandstone bodies are repeatedly separated by thin shaly-sand and shale intervals. Consequently, reservoir-quality sand bodies have substantially greater potential for lateral linkage than for uninterrupted vertical communication. The identical major and minor horizontal variogram ranges indicate that the fitted model does not establish a preferred horizontal direction; consequently, the lateral sand-body orientations illustrated in Figure 6 are interpreted from facies geometry rather than variogram-derived directional anisotropy.

The SIS facies illustrations are consistent with possible lateral linkage of sand bodies and local vertical separation by shale. They do not establish the fraction of sand connected within either interval.

The horizontal-to-vertical variogram-range ratio indicates strong anisotropy in modelled spatial correlation. Variogram ranges alone cannot quantify connected sand volume, hydraulic communication, or the number of reservoir compartments.

The available results are consistent with the hypothesis that facies architecture and anisotropy may influence potential static connectivity. However, this hypothesis has not been quantitatively tested using connected-component statistics, and dynamic communication remains unverified.

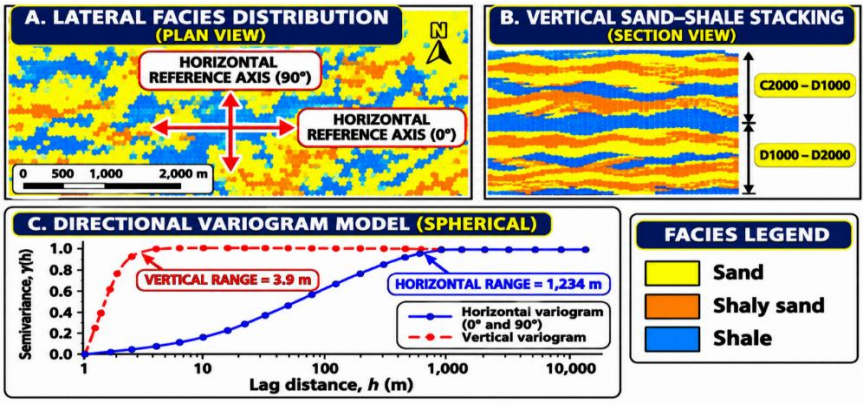


Figure 5. Schematic illustration of lateral facies distribution (A), vertical sand–shale stacking (B), and directional spherical variogram models (C) for the Chinak Field. The horizontal and vertical variogram ranges are 1,234 m and 3.9 m, respectively. The 0° and 90° axes represent orthogonal horizontal reference directions without preferential anisotropy. The schematic variogram curves

illustrate spatial correlation rather than measured reservoir connectivity and do not represent original experimental variogram data

Comparative controls on reservoir connectivity and compartmentalization

The displayed models suggest relatively more persistent and stacked sand bodies in C2000–D1000 and greater channel-scale variability and lateral termination in D1000–D2000. These visual differences indicate possible contrasts in static geological connectivity but cannot establish measured compartment counts or connected sand fractions.

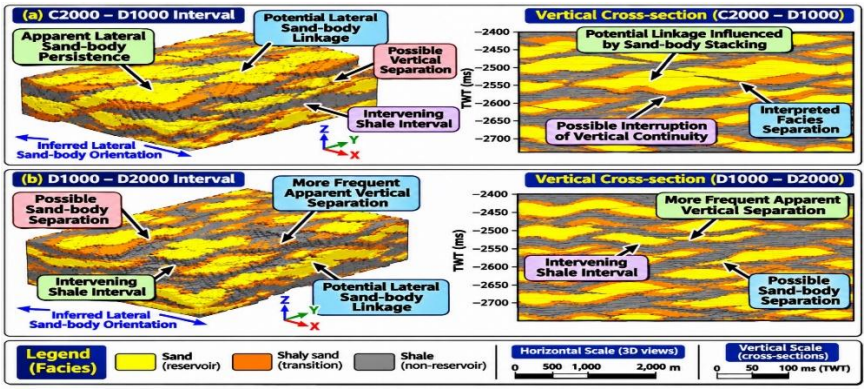


Figure 6. Comparative conceptual interpretation of potential static geological connectivity in the C2000–D1000 and D1000–D2000 reservoir intervals, Chinak Field, onshore Niger Delta. The three-dimensional facies illustrations and corresponding vertical cross-sections highlight differences in sand-body geometry, lateral persistence, vertical stacking, and the distribution of intervening shaly-sand and shale facies. The C2000–D1000 interval suggests potentially more persistent lateral sand-body linkage, whereas the D1000–D2000 interval displays greater apparent variability in sand-body geometry and possible separation by non-reservoir facies. These interpretations are qualitative and do not represent measured connected sand volumes, confirmed compartment boundaries, or demonstrated hydraulic communication. The arrows indicating inferred lateral sand-body orientation represent qualitative interpretations of the displayed facies geometry and do not indicate a preferred horizontal direction established by variogram analysis.

The comparative facies illustrations suggest differences in the potential static geological connectivity of the two reservoir intervals. The C2000–D1000 interval displays relatively persistent and locally stacked sand bodies, suggesting possible lateral linkage. In contrast, the D1000–D2000 interval exhibits greater apparent variability in sand-body geometry, with intervening shaly-sand and shale facies that may interrupt lateral and vertical continuity. These observations indicate that sand-body geometry, facies stacking, and the distribution of non-reservoir intervals may influence reservoir compartmentalization. However, the absence of cell-level connectivity measurements prevents confirmation of connected sand volumes, compartment boundaries, or effective hydraulic communication. The interpretations therefore represent geological hypotheses that require further evaluation using quantitative connectivity analysis and independent dynamic reservoir data.

Limitations of the Study

The distinction between sand-body connectivity and connectivity to wells (Larue & Hovadik, 2006), together with the capacity of different geological simulations to represent different spatial patterns (Strebelle, 2002), reinforces the need for explicit connected-component analysis and realization-specific uncertainty assessment in future work.

The principal limitation is the absence of the original cell-level three-dimensional SIS facies grids and realization-specific outputs. Consequently, this study could not calculate facies proportions from active cells, connected-component counts, the size or volume of the largest connected sand body, connected sand fractions, or uncertainty across stochastic realizations. Available NTG ranges and variogram correlation lengths quantify reservoir-property variation and spatial correlation, respectively, but neither directly measures reservoir connectivity. Interpretations of lateral linkage and vertical compartmentalization therefore remain qualitative and model-based. Furthermore, the absence of pressure, production, and tracer observations prevents validation of dynamic fluid communication. Future

research should analyse the original Petrel grid exports using a documented face-adjacency criterion and test the resulting static connectivity predictions against independent dynamic data.

CONCLUSION

This study integrates stochastic facies-model interpretations and quantitative spatial-correlation parameters to examine potential static geological connectivity in the stacked C2000–D1000 and D1000–D2000 intervals. The available models suggest sand-body linkage and possible compartmentalization, but connected sand volumes were not measured.

The fitted horizontal and vertical variogram ranges of 1,234 m and 3.9 m yield a horizontal-to-vertical ratio of approximately 316.4, indicating pronounced anisotropy in spatial correlation. This ratio must not be interpreted as a direct measurement of reservoir connectivity.

The reported NTG ranges are 0.53882–0.95224 for C2000–D1000 and 0.47117463–0.99902231 for D1000–D2000. The facies illustrations suggest comparatively persistent sand bodies in the former and more channel-scale variability in the latter; these remain qualitative interpretations.

The findings support the value of integrating facies architecture and spatial anisotropy when assessing potential reservoir connectivity. They do not confirm connected sand volumes, static compartment counts or dynamic fluid communication.

Future work should retrieve the original active-cell Petrel facies grids and realization identifiers, calculate connected-component counts and volume-weighted connected sand fractions, and report uncertainty across realizations. Pressure or production data would then be needed to test whether predicted geological pathways correspond to effective flow communication.

REFERENCES

Adeogun, O. Y., Ajewole, S. O., Folohunsho, O. Y., Adeoti, L., & Adelaja, A. T. (2025). Structural and 3D seismic attribute analysis for reservoir characterization in Pearl Field, offshore Niger Delta. *Discover Geoscience*, *3*, Article 42. https://doi.org/10.1007/s44288-025-00150-5

Al-Mudhafar, W. J., Vo Thanh, H., Wood, D. A., & Min, B. (2024). Stochastic lithofacies and petrophysical property modeling for fast history matching in heterogeneous clastic reservoir applications. *Scientific Reports*, *14*, Article 22. https://doi.org/10.1038/s41598-023-50853-3

Attouman, K. D. B., Adeleye, M. A., Osinowo, O. O., Nwakanma, A., & Agathe, Z. T. (2025). Reservoir description and modelling using integrated seismic and petrophysical data in AKDB field, offshore Niger Delta, Nigeria. *Discover Geoscience*, *3*, Article 176. https://doi.org/10.1007/s44288-025-00292-6

Deutsch, C. V., & Journel, A. G. (1998). *GSLIB: Geostatistical software library and user's guide* (2nd ed.). Oxford University Press.

Igonoh, D. A., Emujakporue, G. O., & Inichinbia, S. (2026). Reservoir characterization using integrated petrophysical evaluation, seismic attributes, and AVO modeling in JASMI Field, Niger Delta Basin. *Nigerian Journal of Physics*, *35*(4), 42–58. https://doi.org/10.62292/njp.v35i4.2026.641

Jin, J., Li, S., Li, J., & Ding, F. (2024). Geological model calibration based on gradual deformation and connectivity function. *Scientific Reports*, *14*, Article 29395. https://doi.org/10.1038/s41598-024-80363-9

Journel, A. G. (1983). Nonparametric estimation of spatial distributions. *Mathematical Geology*, *15*(3), 445–468. https://doi.org/10.1007/BF01031292

Kuye, D. A., & Hampson, G. J. (2023). Sedimentological and tectono-stratigraphic characterisation of a shallow-marine reservoir, 'Dona' field, offshore Niger Delta. *Marine and Petroleum Geology*, *158*, Article 106517. https://doi.org/10.1016/j.marpetgeo.2023.106517

Larue, D. K., & Hovadik, J. (2006). Connectivity of channelized reservoirs: A modelling approach. *Petroleum Geoscience*, *12*(4), 291–308. https://doi.org/10.1144/1354-079306-699

Manzocchi, T., Walsh, D. A., Carneiro, M., & López-Cabrera, J. (2023). Compression-based facies modelling. *Mathematical Geosciences*, *55*, 625–644. https://doi.org/10.1007/s11004-023-10048-y

Olaoluwa, A., Alabi, O. O., Ojo, B. T., & Sedara, S. O. (2025). Enhancement of reservoir characterization with petrophysical analysis of well log data in the "Abig" oil field, Niger Delta, Nigeria. *Nigerian Journal of Physics*, *34*(4), 71–81. https://njp.nipngr.org/index.php/njp/article/view/451

Oyesomi, H. A., Oladele, S., Oyedele, K. F., Adeogun, O. Y., & Omolaiye, G. E. (2025). Siliciclastic reservoir characterisation and geometric trend modelling for hydrocarbon quantification and uncertainty analysis: A case study of Doma Field, Niger Delta Basin, Nigeria. *NRIAG Journal of Astronomy and Geophysics*, *14*(1), 1–17. https://doi.org/10.1080/20909977.2025.2460326

Pyrcz, M. J., & Deutsch, C. V. (2014). *Geostatistical reservoir modeling* (2nd ed.). Oxford University Press.

Reijers, T. J. A. (2011). Stratigraphy and sedimentology of the Niger Delta. *Geologos, 17*(3), 133–162. https://doi.org/10.2478/v10118-011-0008-3

Short, K. C., & Stäuble, A. J. (1967). Outline of geology of Niger Delta. *AAPG Bulletin, 51*(5), 761–779. https://doi.org/10.1306/5D25C0CF-16C1-11D7-8645000102C1865D

Spina, V., Olagundoye, O., Chizea, C., Pellettier, J., Onyeanuna, C., Parsa, A., Joubert, T., Fashanu, M., Enuma, C., Ifihan, J. J., Epelle Ebenezer Seth, E. E., & Olabiyi, T. (2023). Unravelling the impact of geological heterogeneities in reservoir management: An integrated study of the deep-water Akpo Field, Niger Delta. *Marine and Petroleum Geology, 150*, Article 106132. https://doi.org/10.1016/j.marpetgeo.2023.106132

Spina, V., Amoyedo, S., Wibberley, C. A. J., Tozer, R., Ribes, C., Maia, R., Atoyebi, H., & Vincent, E. (2025). Characterization of a deep-water turbiditic reservoir under an active hydrodynamic regime (Niger Delta). *Marine and Petroleum Geology, 172*, Article 107185. https://doi.org/10.1016/j.marpetgeo.2024.107185

Strebelle, S. (2002). Conditional simulation of complex geological structures using multiple-point statistics. *Mathematical Geology, 34*(1), 1–21. https://doi.org/10.1023/A:1014009426274